

12

Permanent-Magnet Synchronous Machine Drives

Patrick L. Chapman
*University of Illinois
at Urbana-Champaign*

- 12.1 [Introduction](#)
- 12.2 [Construction of PMSM Drive Systems](#)
- 12.3 [Simulation and Model](#)
- 12.4 [Controlling the PMSM](#)
Current-Based Drives • Voltage-Based Drives
- 12.5 [Advanced Topics in PMSM Drives](#)

12.1 Introduction

The permanent-magnet synchronous machine (PMSM) drive has emerged as a top competitor for a full range of motion control applications [1–3]. For example, the PMSM is widely used in machine tools, robotics, actuators, and is being considered in high-power applications such as vehicular propulsion and industrial drives. It is also becoming viable for commercial/residential applications. The PMSM is known for having high efficiency, low torque ripple, superior dynamic performance, and high power density. These drives often are the best choice for high-performance applications and are expected to see expanded use as manufacturing costs decrease. The purpose of this chapter is to introduce the PMSM and the application of power electronics technology to its control.

The PMSM is sometimes referred to as a permanent-magnet AC (PMAC) machine or simply as a PM machine. In some instances it is referred to as a brushless DC (BDC) machine because by appropriate control it can be made to have input/output characteristics much like a separately excited brush-type DC machine. It can also take on similarity with the DC machine when Hall effect sensors are utilized for position sensing, whereby electronic, instead of brush, commutation take place. The BDC machine, which is discussed in detail in Chapter 10, is a special case of the more general PMSM drive. The PMSM is a synchronous machine in the sense that it has a multiphase stator and the stator electrical frequency is directly proportional to the rotor speed in the steady state. However, it differs from a traditional synchronous machine in that it has permanent magnets in place of the field winding and otherwise has no rotor conductors.

The use of permanent magnets in the rotor facilitates efficiency, eliminates the need for slip rings, and eliminates the electrical rotor dynamics that complicate control (particularly vector control). The permanent magnets have the drawback of adding significant capital cost to the drive, although the long-term cost can be less through improved efficiency. The PMSM also has the drawback of requiring rotor position feedback by either direct means or by a suitable estimation system. Since many other high-performance drives utilize position feedback, this is not necessarily a disadvantage. Another disadvantageous aspect of the PMSM is cogging torque, which is the parasitic tendency of the rotor to align at

discrete positions due to the interaction of the magnets and the stator teeth. Cogging torque is particularly troublesome at low speed, but can be virtually eliminated either by appropriate design of the machine or by electronic mitigation.

12.2 Construction of PMSM Drive Systems

As stated, the PMSM consists of a multiphase stator and a rotor with permanent magnets. The machines can have either radially or axially oriented flux. Some common radial-flux rotor configurations are depicted in Fig. 12.1. The magnets can be either mounted on the rotor surface (Fig. 12.1a) or buried in the rotor iron (Fig. 12.1b). The surface-mounted variety is popular because of the simplicity of construction and control, and virtual absence of reluctance torque since the stator inductance is essentially independent of rotor position. The buried magnet (or “interior magnet”) variety of rotors has significant reluctance torque due to position-variant stator inductance that complicates analysis and control issues. However, the magnetic saliency can be used advantageously for operation above base speed. There are also variations of the stator design that are possible, particularly in regard to slot skewing and tooth shape. There is a wide variety of motor designs, each of which has its own performance and cost considerations.

There are several different magnet materials that are commonly used. Ferrite is an inexpensive but less magnetically powerful material that is frequently used. The rare earth magnets neodymium-iron-boron (NdFeB) and samarium-cobalt (SmCo) magnets are stronger magnetically and more resistant to temperature. SmCo magnets are particularly resistant to temperature but are comparably very expensive. Sintered NdFeB magnets have a stronger residual field and lower cost than SmCo magnets, but are less temperature resistant. Bonded NdFeB magnets are not quite as strong as SmCo, but are less expensive and are more easily shaped. Ferrite magnets are very common for lower-performance motors. Both radial and parallel magnetization are commonly used, depending on application. The particular choice of magnets and other design factors is important, but does not directly influence the basic principles of power converter control.

The multiphase stator is much like the stator of any other AC machine. Frequently, the slot design is distinctive in that measures are taken to reduce cogging torque. Use of tooth “shoes” and slot skewing is prevalent. Although distributed windings are common, lumped windings are also used when it is desired to have an approximately “trapezoidal” back emf. Advances are being made in the area of slotless (i.e., “toothless”) PMSM design as well [4].

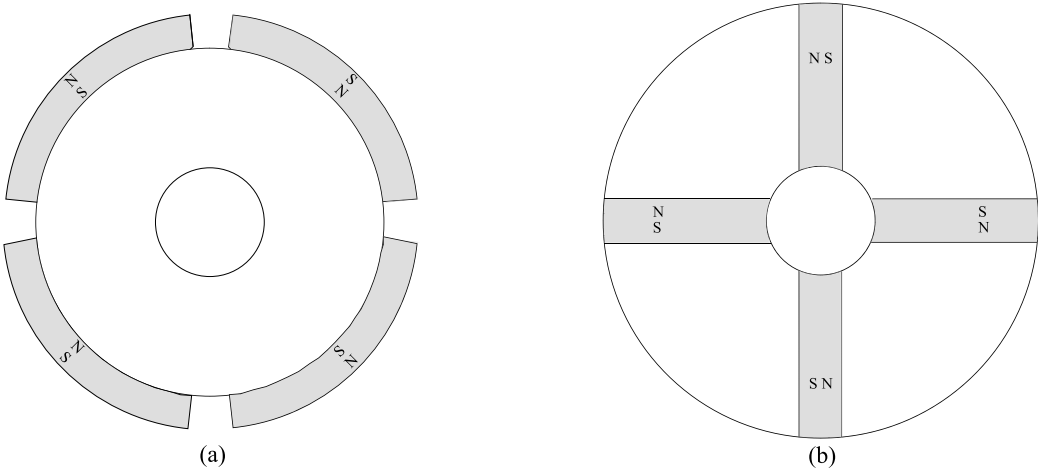


FIGURE 12.1 Typical PMSM rotor configurations: (a) surface-mount; (b) buried.

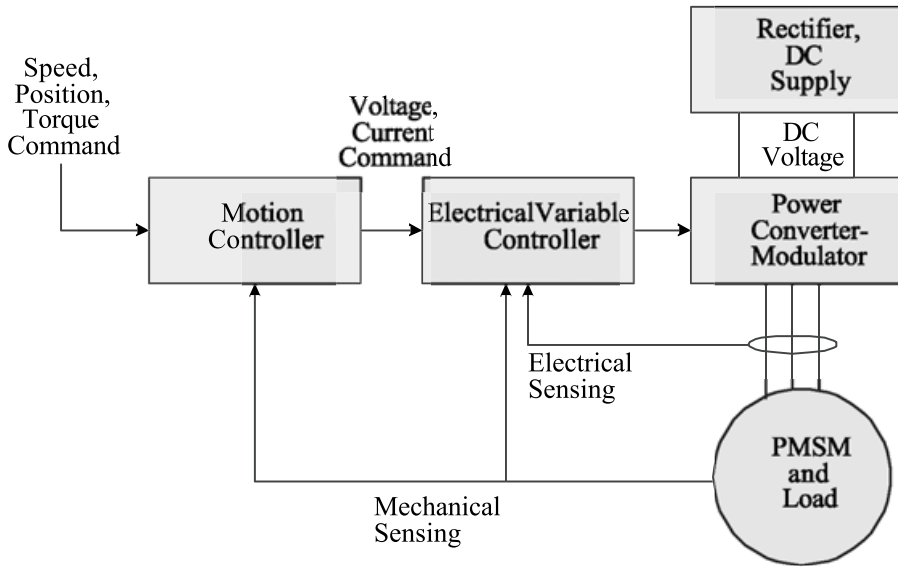


FIGURE 12.2 Diagram of conceptual drive system.

The aspects of motor construction that most significantly influence power converter design are the shape of the back emf, the cogging torque, the magnetic saliency (surface-mount or buried magnets), and the power requirements. Any of the standard inverter topologies discussed in Chapters 5 and 6 can be used to drive the machine. A conceptual drive system is pictured in Fig. 12.2. There, a speed, position, or torque command is input to the drive system. The motion controller implements feedback control based on mechanical sensors (or estimators). The controller outputs commands for the electrical variables to obey. The electrical control block converts its input commands into commands for the power converter/modulator block and sometimes utilizes feedback of voltage or current. The power converter block imposes the desired electrical signals onto the PMSM machine with the connected load.

12.3 Simulation and Model

When designing a PMSM drive, it is useful to compose a computer simulation before building a prototype. Such a model can also be used to develop the control. A suitable model of the PMSM is set forth in this section. Much of the detail of development is omitted because it is not the purpose of this chapter to provide derivations, but simply to provide the reader with useful formulas for designing the electronics for PMSM drive systems. Full development of PMSM drive models is available from a number of references [1, 2].

If there are N phases, then there are N stator voltages, currents, and flux linkages. Let the set of stator voltages be represented compactly as

$$\mathbf{v} = [v_1 \quad v_2 \quad \cdots \quad v_N]^T \quad (12.1)$$

where v_x is the voltage across the x th phase. The same relationship holds for the vectors of current (\mathbf{i}), and flux linkage (λ). For the special and common case of three-phase machines, the letters a , b , and c are used in place of 1, 2, and 3, respectively, in Eq. (12.1).

Since eddy current and hysteresis losses are generally small, it will suffice to attribute all stator losses to the winding resistance, r . Then, applying Faraday's and Ohm's laws, the stator voltage equation may

be written as

$$\mathbf{v} = r\mathbf{i} + \frac{d}{dt} \boldsymbol{\lambda} \quad (12.2)$$

Regarding the machine as balanced, symmetrical, and magnetically linear, the flux linkage equation may be written as

$$\boldsymbol{\lambda} = \mathbf{L}\mathbf{i} + \boldsymbol{\lambda}_{\text{pm}} \quad (12.3)$$

where \mathbf{L} is a symmetric $N \times N$ matrix of the appropriate self- and mutual inductances and $\boldsymbol{\lambda}_{\text{pm}}$ is an $N \times 1$ vector of stator flux linkages due to the permanent magnet. The inductance matrix is constant for machines with surface-mounted magnets, but has rotor position-dependent terms for machines with buried magnets.

The torque equation can be derived from coenergy relationships:

$$T_e = \frac{P}{2} \frac{\partial}{\partial \theta_r} \left(\frac{1}{2} \mathbf{i}^T \mathbf{L} \mathbf{i} + \mathbf{i}^T \boldsymbol{\lambda}_{\text{pm}} \right) + T_{\text{cog}} \quad (12.4)$$

where θ_r is the electrical rotor position in radians, and P is the number of poles. Mechanical rotor position is $\theta_{\text{rm}} = 2\theta_r/P$. The cogging torque is represented as T_{cog} .

Equations (12.2) to (12.4) represent a simulation model of the machine, provided that the resistance, r , the inductance matrix, \mathbf{L} , the cogging torque, T_{cog} , and the permanent magnet flux linkage vector, $\boldsymbol{\lambda}_{\text{pm}}$, are known. The parameters can be determined from direct measurement or by calculation from motor geometry (i.e., finite-element analysis). The mechanical dynamics of the system, which are not discussed here since they can widely vary, must be simulated to determine position and speed.

The model set forth is general for any number of phases and for the buried or surface-mounted magnet cases. For a surface-mounted magnet machine, the air gap is effectively very wide and uniform since the magnet material has a relative permeability near 1. This results in stator inductance, which is generally not dependent upon rotor position. In both the surface-mount and buried magnet cases, $\boldsymbol{\lambda}_{\text{pm}}$ is a function of rotor position. Therefore, the torque equation for the surface-mounted case is

$$T_{e(\text{SM})} = \frac{P}{2} \mathbf{i}^T \frac{\partial}{\partial \theta_r} \boldsymbol{\lambda}_{\text{pm}} + T_{\text{cog}} \quad (12.5)$$

and the torque equation for a machine with buried magnets is

$$T_{e(\text{BM})} = \frac{P}{2} \mathbf{i}^T \left(\frac{1}{2} \left(\frac{\partial}{\partial \theta_r} \mathbf{L} \right) \mathbf{i} + \frac{\partial}{\partial \theta_r} \boldsymbol{\lambda}_{\text{pm}} \right) + T_{\text{cog}} \quad (12.6)$$

where it is noted that the current, \mathbf{i} , is not explicitly dependent on rotor position.

The cogging torque may be represented as

$$T_{\text{cog}} = \sum_{z \in Z} T_q^z \cos(zN_t \theta_r) + T_d^z \sin(zN_t \theta_r) \quad (12.7)$$

where Z is the set of natural numbers such that the Fourier series constants T_q^z and T_d^z are negligible and the constant, N_t , is the number of stator teeth. The cogging torque is frequently ignored in designing the motor drive electronics or it is sufficiently negligible because of special machine design efforts. If cogging torque is neglected, then the constants T_q^z and T_d^z are zero.

The power into the machine is simply the sum of the power into each phase:

$$P_{\text{in}} = \mathbf{v}^T \mathbf{i} \quad (12.8)$$

and the power output of the machine is

$$P_{\text{out}} = T_e \omega_{\text{rm}} \quad (12.9)$$

where ω_{rm} is the mechanical rotor speed. In Eq. (12.9), the frictional and windage dynamics are assumed to be negligible or to be accounted for in the mechanical system model.

As a common special case of the model in Eq. (12.9), the analysis is restricted to three-phase machines ($N = 3$). Frequently, the back emf of the machine has negligible harmonics, and thus it can be treated as if it is purely sinusoidal. As is common in buried magnet machine analysis, the rotor position variance of the stator inductance can be taken as sinusoidal. Furthermore, the cogging torque can be made small by utilizing certain design techniques. With these assumptions, a transformation of machine variables into the rotor reference frame can be made that facilitates vector control of the PMSM.

If the back emf is sinusoidal, then the flux linkage due the permanent magnets is as well. That is, λ_{pm} may be expressed as

$$\lambda_{\text{pm}} = \lambda_m \left[\sin(\theta_r) \quad \sin\left(\theta_r - \frac{2\pi}{3}\right) \quad \sin\left(\theta_r + \frac{2\pi}{3}\right) \right]^T \quad (12.10)$$

where λ_m is a constant equal to the peak strength of the flux linkage due to the magnets. Note that Eq. (12.10) implies a certain interpretation of the measured rotor position. Specifically, it implies that the magnet flux linking the first phase is zero when $\theta_r = 0$. Then, the back emf due to the permanent magnets may be stated as

$$\mathbf{e}_{\text{pm}} = \omega_r \lambda_m \left[\cos(\theta_r) \quad \cos\left(\theta_r - \frac{2\pi}{3}\right) \quad \cos\left(\theta_r + \frac{2\pi}{3}\right) \right]^T \quad (12.11)$$

where ω_r is the electrical rotor speed and equals $P/2$ times its mechanical counterpart, ω_{rm} . Equation (12.11) is a useful expression for determining the constant λ_m experimentally.

The rotor position-dependent terms can be eliminated by transforming the variables into a reference frame fixed in the rotor. Only the results of this long process are given here. The transformation is applied as

$$\mathbf{v}_{qd0} = \mathbf{K} \mathbf{v} \quad (12.12)$$

where

$$\mathbf{v}_{qd0} = [v_q \quad v_d \quad v_0]^T \quad (12.13)$$

and [Ref. 1]

$$\mathbf{K} = \frac{2}{3} \begin{bmatrix} \cos(\theta_r) & \cos\left(\theta_r - \frac{2\pi}{3}\right) & \cos\left(\theta_r + \frac{2\pi}{3}\right) \\ \sin(\theta_r) & \sin\left(\theta_r - \frac{2\pi}{3}\right) & \sin\left(\theta_r + \frac{2\pi}{3}\right) \\ \frac{1}{2} & \frac{1}{2} & \frac{1}{2} \end{bmatrix} \quad (12.14)$$

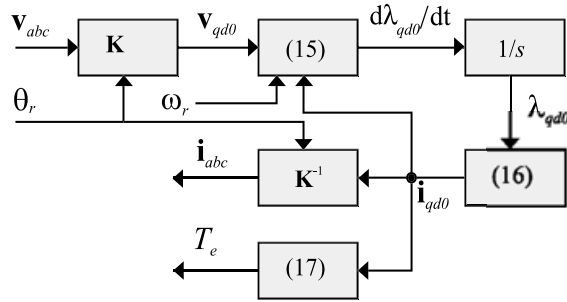


FIGURE 12.3 Diagram of simulation model.

Similar relationships hold for flux linkage and current by replacing v with λ and i , respectively.

After transforming the equations into the rotor reference frame with Eq. (12.14), the following relationships hold:

$$\begin{aligned} v_q &= r i_q + \omega_r \lambda_d + \frac{d}{dt} \lambda_q \\ v_d &= r i_d - \omega_r \lambda_q + \frac{d}{dt} \lambda_d \\ v_0 &= r i_0 + \frac{d}{dt} \lambda_0 \end{aligned} \quad (12.15)$$

$$\begin{aligned} \lambda_q &= L_q i_q \\ \lambda_d &= L_d i_d + \lambda_m \\ \lambda_0 &= L_0 i_0 \end{aligned} \quad (12.16)$$

$$T_e = \frac{3}{2} \frac{P}{2} \lambda_m i_q + (L_d - L_q) i_d i_q \quad (12.17)$$

where L_q , L_d , and L_0 are constant inductances, which are obtainable from measurement from finite-element analysis. In general, the inductance values are not very high, since the flux due to stator current is predominantly leakage, due to the effectively wide air gap.

It is important to note that for the surface-mounted machine, $L_d = L_q$ because the stator inductances are independent of rotor position. This eliminates the second term in Eq. (12.17). For buried magnet motors, by the convention given $L_q > L_d$ in general because the high-permeability paths are aligned with the q -axis. Also, it is common to wye-connect the three phases. In that case, $i_0 = 0$ and therefore both $\lambda_0 = 0$ and $v_0 = 0$ thereby eliminating the zero-sequence components completely. Under constant torque and speed conditions, each current, flux linkage, and voltage are also constant in Eqs. (12.15) to (12.17). Equations (12.15) to (12.17) represent a standard model for a PMSM with sinusoidal flux linkages for either the surface-mounted or buried magnet cases. A diagram of the simulation structure is shown in Fig. 12.3, where numbers in parentheses refer to equation numbers.

12.4 Controlling the PMSM

There are many ways to use power converters to fix the voltage or current in a PMSM drive to desired set points. Chapter 7 details the modulation methods for inverter control. Among them are voltage control methods (such as six-step, sinusoidal, and space-vector modulation) and current control methods (such as hysteresis and delta modulation). There are also methods that augment the basic modulation strategies

to ensure that the desired voltage or current is reached in the steady state (such as a synchronous current regulator). Because these topics are covered elsewhere in the book, the details are omitted in this chapter. In this section, the appropriate voltage and current commands are discussed. These commands become the inputs to the power electronics converter with the given modulation strategy. The specific topology of the inverter also can vary widely, such as the standard fully controlled bridge, H-bridge, ARCP converters, multilevel converters, etc.

Current-Based Drives

Current-based PMSM drives are typically used in motion control systems where a commanded torque is generated. It is not attempted in this chapter to develop the control loops associated with the mechanical apparatus. Rather, the focus is on the electrical aspects of the drive with specific emphasis on developing the appropriate torque. In particular, the current command can be derived directly from the torque equation.

Let the commanded torque be designated as T_e^* . By using the machine equations that were transformed into the rotor reference frame, other useful formulas can be developed. For example, the surface-mounted three-phase machine current command is simply

$$i_q^* = \frac{T_e^*}{\frac{3}{2} \frac{P}{2} \lambda_m} \quad (12.18)$$

where the actual phase currents would then be calculated from applying the inverse transformation of Eq. (12.14) to the vector $[i_q^* \ 0 \ 0]^T$. Note that for a constant torque command, i_q^* is constant. This relationship can also be used for the buried magnet case, but is not optimal for efficiency. If machines with nonsinusoidal back emf are considered, then the reader is referred to Refs. 5 and 6.

The buried magnet case is significantly more complicated. However, the current command that minimizes stator rms current for a given torque is

$$i_q^* = \frac{T_e^*}{\frac{3}{2} \frac{P}{2} \lambda_m + (L_d - L_q) i_d^*} \quad (12.19)$$

where the commanded d -axis current is obtain from solving

$$i_d^* \left(\frac{3}{2} \frac{P}{2} \lambda_m + (L_d - L_q) i_d^* \right)^2 + T_e^* (L_d - L_q) = 0 \quad (12.20)$$

numerically. The result could be stored as a table vs. torque command for application purposes.

As the speed of the machine increases, so does the back emf. At some speed there is no longer enough voltage available for the inverter to supply the current commanded by Eqs. (12.18) through (12.20). To increase the speed beyond this point, field (or “flux”) weakening must be employed [7–10]. That is, the current must be adjusted to reduce the back emf and maintain the desired power. At rated torque and speed, the rms current is at its limit. Field weakening can be employed to increase the motor speed while holding the rms current constant and de-rating the torque, thereby maintaining a large constant power range (Fig. 12.4). There are a variety of methods to accomplish this task, each with its own restrictions, advantages, and complexity. The method is more effective for the buried magnet machine since the d -axis current can produce torque. As an example, the example for the qd model above is continued.

The peak phase voltage required may be expressed as

$$v_s = \sqrt{v_q^2 + v_d^2} \quad (12.21)$$

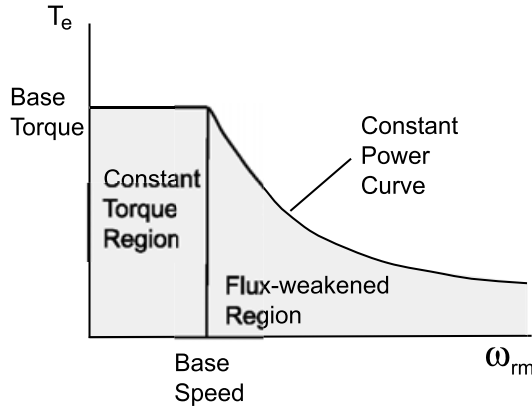


FIGURE 12.4 Torque–speed curve of a flux-weakened PMSM drive.

which cannot be in excess of the voltage that the inverter can supply.

The transformation to the rotor reference frame has the convenience that when steady state is reached, the state variables are constant. Therefore, the qd voltages can be written as

$$\begin{aligned} v_q &= r i_q^* + \omega_r (L_d i_d^* + \lambda_m) \\ v_d &= r i_d^* - \omega_r L_q i_q^* \end{aligned} \quad (12.22)$$

from which the required phase voltage, Eq. (12.23), may be calculated. For the surface-mounted case, this constrained problem can be solved explicitly and the current commands above base speed can be written functionally. However, it cannot be solved explicitly for the buried magnet case. In general, it is perhaps most appropriate in this approach is to build a data set of current commands vs. torque and speed regardless of the structure of the machine.

This method of building the current commands relies heavily on machine parameterization. Advanced methods utilize closed-loop methods to eliminate or drastically reduce the dependence on parameters. However, they are too numerous to cover adequately here, and the reader is referred to the literature. Indeed, advanced control methods for PMSM drives is still an active research area.

Once the current commands have been developed for a given commanded torque, they can be directly issued to a current-regulated inverter. For example, either hysteresis or delta modulation could be used to achieve a good approximation to the desired current waveform. These techniques will cause the current to rise very quickly to the desired value, resulting in high-bandwidth torque control, limited only by the stator time constant and available voltage. If the command is sinusoidal, there are methods to ensure that the exact fundamental component is achieved in the steady state, such as the synchronous current regulator [11]. If nonsinusoidal current is used in case of nonsinusoidal back emf, a synchronous current regulator cast in multiple reference frames can be utilized to achieve steady-state convergence [12].

Voltage-Based Drives

It is not uncommon to utilize a voltage-based control rather than a direct current control. Voltage control PWM techniques can have preferable performance over current-based techniques like hysteresis or delta modulation. Because the torque is not an explicit function of voltage as it is for current, voltage control is not quite as straightforward.

One approach to voltage control is to begin with a torque command and synthesize a current command, as was done above. Then, use a current control loop to drive the phase currents to the appropriate values, thus achieving the desired torque. For example, if the current commands are formulated in the rotor

reference frame as i_q^* and i_d^* :

$$\begin{aligned} v_q^* &= \omega_r(L_d i_d + \lambda_m) + (K_p + K_i/s)(i_q^* - i_q) \\ v_d^* &= -\omega_r L_q i_q + (K_p + K_i/s)(i_d^* - i_d) \end{aligned} \quad (12.23)$$

where K_p and K_i are the proportional and integral control constants, respectively. The Laplace operator is s . Assuming that the voltage commanded is the voltage obtained, the transfer function between the commanded and actual current is

$$\frac{i_q}{i_q^*} = \frac{\frac{K_p}{L_q} \left(s + \frac{K_i}{K_p} \right)}{s^2 + \frac{r + K_p}{L_q} s + \frac{K_i}{L_q}} \quad (12.24)$$

where the same relationship holds if q is replaced with d . By utilizing this expression, the poles and zero of the current control can be arbitrarily set. In the steady state, the desired current, and therefore torque, is obtained. This method is common despite the inherent parameter dependence of pole placement.

Another example of PMSM control by voltage-based operation is a direct speed control. For example, the duty-cycle command given to the voltage source inverter could be formulated as

$$d = (K_p + K_i/s)(\omega_{rm}^* - \omega_{rm}) \quad (12.25)$$

where ω_{rm}^* is the commanded speed. This control is simple, requires little in the area of sensors, and will ensure steady-state realization of the desired speed. It can, however, suffer from overmodulation and result in a comparatively sluggish control. By itself, Eq. (12.25) generally does not result in currents that obtain maximize efficiency. An additional control would need to be added to control the phase angle of the voltage.

Several variations on both current- and voltage-based control can be found in the literature. The methods presented only represent an introduction to these topics, and the reader is encouraged to investigate several other alternatives [13].

12.5 Advanced Topics in PMSM Drives

There are a large number of possible avenues for advancement of control of PMSM drives. A major research area is that of sensorless control [14–16]. This typically means that measures have been taken to eliminate the expensive rotor position sensor, but not necessarily current or voltage sensors. By employing estimation methods, a satisfactory measure of rotor position can often be obtained at minimal cost and added complexity.

Operation of the machine above base speed is of particular interest in vehicular propulsion applications. For this reason, many engineers have investigated field-weakening controls that extend the speed range of machine by effectively reducing the magnet flux [7–10]. This was briefly mentioned above, yet is an extensive topic with many challenges.

Many of the control systems set forth have parameter-dependent formulations. With time, wear, and temperature, the machine parameters can vary significantly, negatively affecting system performance. Therefore, the topic of dynamic parameter estimation is also an active research area.

Another area of active research is that of active vibration suppression. By prudent operation of the power converter, it is possible to manipulate the torque to mitigate ripple. There is also exploratory research in the area of mitigating nontorsional vibration as well. Adaptive controls, neural nets, and a host of other advanced topics in automatic control can also be applied to PMSM drives.

In short, the PMSM motor drive is a effective in high-performance drive applications. Rapid torque response is readily achieved as vector control of PMSM drives is much more straightforward than it is for induction motor drives. The capital cost can be high, but the high efficiency can at least partially offset this in high-power applications. For these reasons, the PMSM drive is expected to continue to be competitive for the near future.

References

1. P. C. Krause, O. Wasynczuk, and S. D. Sudhoff, *Analysis of Electric Machinery*, IEEE Press, Piscataway, NJ, 1996.
2. P. Pillay and R. Krishnan, Modeling of permanent magnet motor drives, *IEEE Trans. Ind. Electron.*, 35(4), 537–541, 1988.
3. B. K. Bose, Ed., *Power Electronics and Variable Frequency Drives*, IEEE Press, Piscataway, NJ, 1997, chap. 6.
4. D. C. Hanselman, *Brushless Permanent-Magnet Motor Design*, McGraw-Hill, New York, 1994.
5. P. L. Chapman, S. D. Sudhoff, and C. A. Whitcomb, Optimal current control strategies for surface-mounted permanent-magnet synchronous machine drives, *IEEE Trans. Energy Conversion*, 14(4), 1043–1050, 1999.
6. D. C. Hanselman, Minimum torque ripple, maximum efficiency excitation of brushless permanent magnet motors, *IEEE Trans. Ind. Electron.*, 41(3), 292–300, 1994.
7. S. D. Sudhoff, K. A. Corzine, and H. J. Hegner, A flux-weakening strategy for current-regulated surface-mounted permanent-magnet machine drives, *IEEE Trans. Energy Conversion*, 10(3), 431–437, 1995.
8. S. R. Macminn and T. M. Jahns, Control techniques for improved high-speed performance of interior PM synchronous motor drives, *IEEE Trans. Ind. Appl.*, 27(5), 997–1004, 1991.
9. A. K. Adnanes and T. M. Undeland, Optimum torque performance in PMSM drives above rated speed, in *Conference Record of the 1991 Industry Applications Society Annual Meeting*, 1991, 169–175.
10. M. F. Rahman, L. Zhong, and K. W. Lim, A DSP based instantaneous torque control strategy for interior permanent magnet synchronous motor drive with wide speed range and reduced torque ripples, in *Conference Record of the Thirty-First Annual Industry Applications Society Meeting*, 1996, 518–524.
11. T. M. Rowan and R. J. Kerkman, A new synchronous current regulator and an analysis of current-regulated drives, *IEEE Trans. Ind. Appl.*, IA-22(4), 678–690, 1986.
12. P. L. Chapman and S. D. Sudhoff, A multiple reference frame synchronous estimator/regulator, *IEEE Trans. Energy Conversion*, 15(2), 197–202, 2000.
13. W. Leohnard, *Control of Electric Drives*, 2nd ed., Springer-Verlag, New York, 1997.
14. K. A. Corzine and S. D. Sudhoff, Hybrid observer for high performance brushless DC motor drives, *IEEE Trans. Energy Conversion*, 11(2), 318–323, 1996.
15. D. Jung and I. Ha, Low-cost sensorless control of brushless DC motors using a frequency-independent phase shifter, *IEEE Trans. Power Electron.*, 15(4), 742–752, 2000.
16. J. P. Johnson, M. Ehsani, and Y. Guzelgunler, Review of sensorless methods for brushless DC, in *Conference Record of the 1999 Industry Applications Society Annual Meeting*, 1999, 143–150.